RESEARCH

Impact of Rubber Content on Performance of Ultra-High-Performance Rubberised Concrete (UHPRuC)

Thong M. Pham[1], Josh Lee[5], Emad Pournasiri[2,6], Jun Li[2], Zhen Peng[2], Kaiming Bi[3] and Tung M. Tran[4*]

Abstract

This study investigated the effect of rubber content on the mechanical characteristics of ultra-high-performance rubberised concrete (UHPRuC). The results revealed a distinctive non-linear decrease in the dry density of UHPRuC as the rubber content increased. Notably, lower rubber content led to a columnar failure mode, while higher content (≥ 20%) exhibited a mixed failure mode with vertical cracking and diagonal fracture. Importantly, the compressive strength showed minimal reduction compared to conventional concrete, presenting a remarkable 50% mitigation of strength reduction compared to previous studies. Utilising reference concrete with robust bond strength proved highly effective in preserving strength in rubberized concrete. Despite its effectiveness in mitigating compressive strength reduction, UHPC could not effectively offset flexural strength loss, which ranged from 1.5 to 3 times that of compressive strength loss. The addition of rubber aggregate in UHPC reduced the peak flexural strength, residual strength, and flexural toughness at a similar rate, while significantly increasing the vibration decaying rate. Incorporating 40% rubber in UHPRuC reduced the eCO_2 up to 37%. Our findings emphasise the importance of reference concrete with good bond strength and shows that the addition of rubber aggregate in UHPC leads to reductions in strength but increases the energy-dissipating capacity.

Keywords Ultra-high-performance concrete, Rubberised concrete, Damping, Green concrete

*Correspondence:
Tung M. Tran
tranminhtung@tdtu.edu.vn
[1] UniSA STEM, University of South Australia, Mawson Lakes, SA 5095, Australia
[2] Centre for Infrastructural Monitoring and Protection, School of Civil and Mechanical Engineering, Curtin University, Kent Street, Bentley, WA 6102, Australia
[3] Department of Civil and Environmental Engineering, The Hong Kong Polytechnic University, Kowloon, Hong Kong, China
[4] Sustainable Developments in Civil Engineering Research Group, Faculty of Civil Engineering, Ton Duc Thang University, Ho Chi Minh City, Viet Nam
[5] Roads and Civil Infrastructure, Transport Group, GHD Pty Ltd, Perth, Australia, WA 6000
[6] Engineering Department, Parma Composites, 14 Garino Rise, WA 6065 Perth, Australia

1 Introduction

Waste management of non-biodegradable materials remain a pressing global challenge. Annually, 1.5 billion new tyres are manufactured, with 1 billion reaching the end of their life cycle, and approximately 4 billion used tyres accumulate in stockpiles or landfills (WBCSD, 2010). In Australia, 48.5 million equivalent passenger units (460,000 tonnes) face disposal each year, with only 34% being recycled (Mountjoy and Mountjoy 2012). The consequences include health risks, fire hazards, and resource wastage (WBCSD, 2010). Australia's concrete industry produces over 30 million cubic metres of concrete annually, exceeding 1 m^3/person/year (Cement Concrete & Aggregates Australia, 2022). Australia's concrete industry, producing over 30 million cubic metres annually, seeks to incorporate waste materials like steel fibres, plastic, glass, rubber, and recycled bricks.

Pham *et al. Int J Concr Struct Mater*   (2024) 18:59

Page 2 of 15

Achieving environmentally sustainable concrete while maintaining essential properties is the challenge. Partially replacing aggregates with recycled rubber offers a viable solution—rubberized concrete—derived from processed used tyres (Marinković et al., 2010).

When natural aggregates are partially replaced with rubber aggregates in Portland cement concrete, an increase in concrete ductility but a drastic reduction in the compressive and tensile strengths was found (Eldin & Senouci, 1992; Gesoglu & Guneyisi, 2007). Researchers are increasingly interested in rubberized concrete, aiming for higher performance while leveraging its potential benefits, including lightweight properties, greater damping ratio, and good impact resistance and thermal/acoustic insulation (Feng et al., 2021, 2022; Sun et al., 2023). However, it is essential to acknowledge that rubberized concrete's compressive strength is adversely affected, potentially limiting its structural applications (Bakhoum & Mater, 2022; Elsayed et al., 2022; Feng et al., 2022; Jafarifar et al., 2023). Thus, non-structural elements such as walls, noise barriers, traffic barriers, and paving slabs are recommended applications (Li et al., 2014).

Recent studies attributed performance loss in concrete to inadequate internal bonding between rubber aggregates and the matrix (Bušić et al., 2018; Gravina et al., 2021; Onuaguluchi & Banthia, 2017). Mitigating the strength reduction involves various approaches, e.g. pre-treatment of rubber aggregate, additives to the concrete mix, and optimal rubber content and size (Bušić et al., 2018). These findings suggest the potential for improved rubberised concrete in load-bearing structures. Abdelmonem et al. (2019) produced rubberised concrete with a favourable compressive strength exceeding 40 MPa based on a 60 MPa mix design. The better bonding between matrix and aggregates in the reference concrete contributes to the improved performance of rubberized concrete at lower rubber replacement levels. However, higher rubber replacement resulted in a detrimental strength reduction (Abdelmonem et al., 2019). To address this, utilising reference concrete with strong bonding is proposed as a solution to minimize strength loss when incorporating rubber aggregates.

Ultra-high-performance concrete (UHPC) offers a potential solution for achieving enhanced mechanical performance with rubber aggregates. UHPC is expected to exhibit the compressive strength exceeding 120 MPa (El-Helou et al., 2022; Portland Cement Association, 2023). The addition of rubber aggregates may cause a minimal reduction in the mechanical performance; however, the overall strength of UHPRuC is expected exceeding normal-strength rubberised concrete (NSRuC). There have been no such studies in the literature until recently (Li et al., 2022; Pham et al., 2021a), which only focused on dynamic properties.

As evident from the literature, there is a noticeable absence of studies focusing on the static properties and vibration characteristics of UHPRuC, especially those aiming to optimise strength reduction and enhance the damping index. This study seeks to fill this gap by examining the impact of rubber content on the mechanical properties of UHPRuC, with the goal of achieving minimal strength loss while maximising both its vibration characteristics and rubber inclusion. The embodied carbon dioxide of UHPRuC is also investigated.

2 Literature Review

The mechanical properties of rubberised concrete are affected by many factors including the replacement levels and rubber size. These factors have different effects on the mechanical properties including the compressive strength, flexural strength, elastic modulus, and damping ratio. Varying rubber aggregate size and contents have been studied in previous studies. This section provides a brief review of their effects on the physical and mechanical properties of rubberised concrete.

2.1 Compressive Strength

Eldin and Senouci (1993) compared the compressive strength of rubberised concrete made of two different rubber aggregate groups including 19–38 mm chips and < 1 mm ground rubber at 0, 25, 50, and 75% volumetric replacement ratio. Group 1 replaced natural coarse aggregates with rubber chips, while Group 2 replaced natural sand with ground rubber. The specimens containing rubber chips showed a greater decrease in strength, attributed to the rubber aggregates' low modulus of elasticity causing deformation rather than load-bearing under external forces. This study found a non-linear relationship between compressive strength and rubber volume, with a significant decline up to 50% replacement, followed by stability at higher replacement levels. Results aligned with Popovich' model, indicating the rubber aggregates as voids within the specimens (Eldin & Senouci, 1993).

Audrius et al. (2012) conducted a similar study where three different rubber aggregate sizes including 0–1 mm, 1–2 mm, and 2–3 mm were used to replace fine sand at 5, 10, 20, and 30% by volume. The findings were consistent with those of Eldin and Senouci (1993), where the rubber content and compressive strength followed a non-linear relationship similar to Popovics's model. However, unlike the results in Eldin and Senouci (1993), the largest strength loss was evident with the smallest 0–1 mm aggregates and the least with the 2–3 mm aggregates

(Audrius et al., 2012). This observation was different from a recent study by Pham et al. (2021b) who found that rubberised concrete with smaller rubber particle size exhibited higher compressive strength than that of larger rubber aggregates for the same rubber content, aligning with findings from previous studies (Raffoul et al., 2016; Su et al., 2015). Therefore, it can be concluded that very large tyre chips can cause a detrimental loss in the static compressive strength as compared to those with smaller rubber aggregates. It is worth noting that large rubber aggregates can improve the dynamic energy absorption of rubberised concrete as reported by Pham et al. (2021b), but it is out of the scope of this study.

2.2 Flexural Strength

The flexural strength has been also well examined by previous studies, but there were a few different findings in the literature. Benazzouk et al. (2007) replaced fine sand with 10, 20, 30, 40, and 50% crumb rubber aggregates < 1 mm, and reinforced with polypropylene fibres. The flexural strength of rubberised concrete did not reduce with an increase in rubber content. Instead, the flexural strength increased with the rubber content up to 20% and then it reduced when increasing the rubber content by more than 30%. The optimum rubber content for maximising the flexural strength was between 20 and 30% with a gain of approximately 18%. Benazzouk et al. (2007) suggested that the improvement in the flexural strength could be attributed to the bridging effect of polypropylene fibres and the elastic nature and ductile characteristics of rubber under loading, but no thorough explanation was provided. Similarly, Holmes et al. (2014) also found similar findings where fine aggregates were replaced with 3 mm crumb rubber at 7.5%. The flexural strength of rubberised concrete increased by 18% regarding the reference concrete. A similar explanation was provided as the rubberised concrete beam exhibited ductile failure with higher energy absorption (Holmes et al., 2014).

Contrary to Benazzouk et al. (2007) and Holmes et al. (2014), several studies have reported a decrease in the flexural strength of rubberised concrete. For instance, Thomas and Gupta (2015) observed a linear decrease in flexural strength as the percentage of fine sand aggregate replaced with crumb rubber aggregate increased. At 20% replacement, the control mix had a flexural strength of 5.3 MPa, reducing to 4.0 MPa (24% reduction). Similarly, Ganjian et al. (2009) also reported a flexural strength decrease from 3 to 1.5 MPa (50% reduction) at 10% replacement. These reductions were attributed to weakened bond strength between cement and rubber, potentially causing micro cracks at the interface and accelerating crack widening during flexural loading, thus reducing flexural strength. This trend aligns with the decreased compressive strength resulting from weak bonding.

These contradicting observations on the mechanical properties of rubberised concrete highlight the need for more extensive research to uncover the underlying causes. While reduced bond strength between the matrix and rubber aggregates has been identified as a plausible explanation for both the compressive and flexural behaviour of rubberised concrete, further studies are required to validate this theory. The weak interface between the matrix and rubber particles may cause the formation of micro cracks, leading to a decline in the mechanical properties of the concrete. Thus, there is a need to better understand the behaviour of rubberised concrete and to optimise its use in construction.

2.3 Density and Damping Ratio

The current research on rubberised concrete indicates that there is a linear relationship between the increase in rubber content and a decrease in unit weight. According to Australian Standards, lightweight concrete has a saturated surface dry density between 1800 kg/m^3 to 2100 kg/m^3 (StandardsAustralia, 2018). Accordingly, rubberised concrete can be classified as lightweight concrete with higher rubber replacement levels. Elchalakani (2015) showed a reduction in rubberized concrete density with higher rubber replacement levels, particularly in high-strength concrete, where a non-linear decrease may be attributed to casting errors or uneven rubber aggregate distribution. The replacement of traditional aggregates with rubber leads to an overall weight reduction, dependent on original mix design unit weight and rubber aggregate quantity, though variations may arise from uneven distribution during mixing.

Meanwhile, increasing the content of rubber aggregates in concrete leads to an increase in the damping ratio, which measures the energy dissipation capability of concrete. Xue and Shinozuka (2013) and Habib et al. (2020) observed an increase in the damping ratio of rubberised concrete by 62% and 67% to 91%, respectively. Zheng et al. (2008) found that rubberised concrete with crumb rubber (GR-8) and chip rubber (CR-40) replacement both showed increases in the damping ratio, but with different trends. Rubberised concrete with crumb rubber replacement (GR-8) exhibited an increase (19.2%–75.3%), while those with chip rubber (CR-40) showed an increase (28.6%–144.0%) in the damping ratio as compared to the reference specimen. In addition, GR-8 with 0–30% rubber experienced an increase in damping ratio while its damping ratio decreased when increased the rubber content from 30 to 45%. This observation was attributed to the ineffective interaction

between cement and excessive rubber content in the mix. Zheng et al. (2008) also found that the damping ratio of CR-40 always increased with the rubber content, which is different from GR-8 with smaller-size crumb rubber. This observation indicated that the increase in the damping ratio was not entirely due to the increase in rubber content but the aggregate size, distribution, and many other factors are also at play.

The vibration tests conducted in the reviewed studies provide insight into the damping behaviour of rubberized concrete. The studies show a noticeable improvement in the damping ratio compared to conventional concrete. However, the relationship between the rubber content and damping ratio is not yet clear and requires further investigation. Some studies observed a linear or parabolic increase in the damping ratio with the rubber content, while others noted a decrease in the damping ratio with an excessive rubber. Despite these discrepancies, it can be concluded that increasing the rubber content results in improved damping properties, but it can have a negative impact on the mechanical performance. These studies were mainly focused on normal-strength concrete with a compressive strength less than 30 MPa, leaving a gap in the understanding of rubberized high-strength concrete, particularly ultra-high-performance rubberized concrete (UHPRuC).

2.4 Pre-Treatment Methods for Rubber Aggregates

Pre-treatment method significantly affects the mechanical properties of rubberised concrete. This review justifies the selection of the pre-treatment method in this study. The current literature suggests two main approaches for improving the strength of rubberized concrete, namely, rubber surface pre-treatment and mixture additives. Rubber surface pre-treatment aims to modify the rubber aggregates' surface area, improving bonding with the matrix through cleaning or coating with cement paste. Mixture additives, such as silica fume, fly ash, or metakaolin, enhance overall mechanical performance by modifying packing or forming additional cement gels. Justifying the chosen pre-treatment method is crucial for the study's validity.

The two common methods of surface pre-treatment involve either soaking the rubber aggregate with sodium hydroxide or washing them with tap water. Chou et al. (2007) immersed rubber aggregates in a sodium hydroxide solution for 5 min, resulting in a notable 19% increase in compressive strength compared to a non-treated control sample. This improvement was attributed to the reaction between sodium hydroxide and rubber, enhancing its hydrophilic properties. The increased hydrophilicity strengthened the bond between rubber and matrix, consequently improving the overall

mechanical performance of rubberized concrete (Chou et al., 2007).

In a similar investigation, Najim and Hall (2013) explored the impact of sodium hydroxide (NaOH) pre-treatment on the mechanical properties of rubberized concrete. In addition, this study also evaluated the influence of varying soaking times (20, 40, and 60 min) of rubber aggregates in the sodium hydroxide solution, compared to a control of non-treated rubber aggregates. The control sample had a compressive strength of 32 MPa, while the 20-min soaking treatment showed a slight improvement of 33 MPa. However, longer soaking times (40 and 60 min) resulted in strength declines to 32.0 MPa and 30.5 MPa, respectively. The 20-min treatment was found to chemically modify the rubber surface, enhancing the bond with cement. Extended soaking weakened the rubber's structural integrity, reducing concrete performance. This study also explore water pre-treatment, yielding a 4% increase in compressive strength compared to the 3% increase achieved with the use of sodium hydroxide (Najim & Hall, 2010). While more advanced pre-treatment methods have been reviewed in recent studies, they are not within the scope of this study.

In general, both water soaking and sodium hydroxide (NaOH) pre-treatment are considered as efficient and simple methods to enhance the compressive strength of rubberized concrete. These techniques improve the surface conditions and increase the bond between the rubber aggregates and the matrix. They also do not demand intensive labour or specialised skills. However, there are some differences between the two methods. NaOH pre-treatment has the advantage of shorter treatment time (20 min) compared to water soaking (24 h). NaOH pre-treatment is also more expensive and requires careful handling of the solution due to its potential environmental impact. Results have shown that NaOH pre-treatment offers minor improvement compared to water pre-treatment. In contrast, water soaking is readily available, accessible, and more cost-effective, making it a favourable choice for most users.

2.5 High-Strength Rubberised Concrete and UHPRuC

It is evident that the static properties of rubberized concrete can be influenced by various factors, including the strength of the reference concrete. Currently, there is limited research on rubberized ultra-high-performance concrete (UHPC), making high-strength concrete the closest comparison.

Elchalakani (2015) studied the compressive and flexural strengths of both high and normal-strength concrete rubberised concrete. The control compressive and flexural strengths for normal-strength concrete

were 58.5 MPa and 6.44 MPa, respectively, whereas for high-strength concrete, they were 104.8 MPa and 9.6 MPa. The maximum reduction in the compressive strength for normal-strength concrete was 89.3% at 40% rubberisation, whereas for high-strength concrete it was 85.2%. Similarly, the reduction in flexural strength was 72.04% for normal-strength concrete and 68.95% for high-strength concrete. In a separate study, Audrius et al. (2012) evaluated the influence of rubber replacement on the compressive strength of high-strength concrete (64 MPa) and found that 20% rubberisation resulted in a 31% reduction in compressive strength, consistent with the findings of other studies.

Limited studies on UHPRuC include works by Li et al. (2022) and Pham et al. (2021a). Li et al. (2022) investigated the effect of incorporating crumbed recycled rubber powders incorporation into UHPC. The authors found the addition of rubber powders reduced the flow ability of UHPC but improved the dynamic compressive properties by increasing the tortuosity of cracks and dissipating energy. The results showed that the dynamic strength of UHPC with rubber powders was more sensitive compared to the control mix. In a separate study, Pham et al. (2021a) examined the quasi-static and dynamic compression characteristics of UHPRuC incorporating different volume fractions of rubber powder. The authors found that the strength reduction was less compared to high-strength rubberized concrete (HSRuC) and normal-strength rubberized concrete (NSRuC) for the same rubber content. The dynamic compressive strength and energy absorption of the UHPRuC were found to be sensitive to the strain rate, and the sensitivity increased with the rubber content.

As can be seen from the review above, there is a scarcity of studies on the mechanical properties of rubberised high-strength concrete and rubberised ultra-high-performance concrete, particularly the damping ratio. Further research is required to fully understand the impact of incorporating rubber on the properties of UHPC and to determine its damping properties.

3 Experimental Programme

The present study aimed to investigate the static and dynamic properties of UHPRuC by conducting a series of tests to determine its density, compressive strength, flexural strength, and vibration characteristics. The control mix design of the UHPC, based on previous research (Pournasiri et al., 2022a, b), will be discussed along with the properties and pre-treatment process of rubber aggregates.
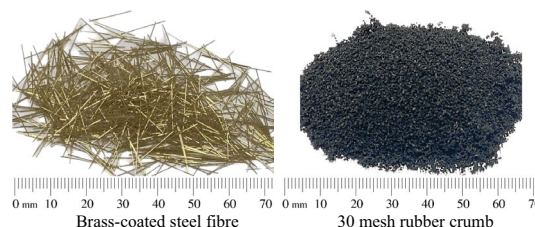

Fig. 1 Steel fibre and rubber aggregates

Fig. 2 Soaking rubber in water for 24 h

3.1 Materials and Mix Design

The study utilised recycled crumb rubber, supplied by Tyre recycle (2018), as a partial replacement for silica sand in UHPC. 30-mesh rubber crumb had a size distribution of 0–0.625 mm with a density of 1,147 kg/m³, which closely matched the size of silica sand. Fig. 1 shows an image of rubber particles. This study used four replacement ratios by volume: 0%, 10%, 20%, and 40%. It is worth noting that larger rubber chips with a size range of 0–14 mm were avoided due to their adverse impact on the strength of concrete, as reported in previous studies (Eldin & Senouci, 1993). The specific gravity of sand was 2.65.

The crumb rubber used as a replacement aggregate underwent a pre-treatment process, including water washing and soaking. Adopted suggestion from Pham et al. (2020), the crumb rubber was soaked for 24 h with a weight placed on top to ensure submersion, using a saturated piece of fabric (see Fig. 2. After the soaking period, the rubber was evenly spread on a large tray and dried in an oven at 60 °C for 2 h, being turned every 30 min to ensure even evaporation until a surface-saturated condition was achieved.

The control UHPC mix consisted of the binder as ordinary Portland cement sourced from Cockburn Cement at 995 kg/m³ with fine aggregates as silica sand and no coarse aggregates. The silica sand was sourced from Cook Industrial Materials with the max particle size of 0.3 mm. The mix was fortified with 238 kg/m³ of silica fume as a strength-enhancing additive, which accounted

Table 1 Mix design of UHPRuC

Mix	UHPRuC_0	UHPRuC_10	UHPRuC_20	UHPRuC_40
Rubber (%)	0	10	20	40
Silica Sand (kg/m^3)	1051	945.9	840.8	630.6
30-mesh rubber (kg/m^3)	0	51.4	102.8	205.7
Cement (kg/m^3)	995	995	995	995
Superplasticizer (kg/m^3)	67	67	67	67
Silica Fume (kg/m^3)	238	238	238	238
Steel Fibre (kg/m^3)	156	156	156	156
Water (kg/m^3)	180	180	180	180
(eCO$_2$) (kgCO$_2$/m^3)	1311	1189	1067	823

Table 2 Physical properties of rubber powder (Pham et al., 2020, 2018)

Mechanical Property	Value
Specific gravity (crumb rubber)	0.54
Fineness modulus (crumb rubber)	2.36%
Water absorption % (crumb rubber)	85%
Young's modulus @100% (truck tyre rubber)	1.97 MPa
Young's modulus @ 300% (truck tyre rubber)	10 MPa
Young's modulus @ 500% (truck tyre rubber)	22.36 MPa
Resilience @ 23 °C (truck tyre rubber)	44%
Resilience @ 75 °C (truck tyre rubber)	55%
Tension strength (truck tyre rubber)	28.1 MPa
Break point strain (truck tyre rubber)	590%

for roughly 23% of the Portland cement and falls within the recommended range of 20–30% as advised by Chan and Chu (2004). The mix was also infused with 180 kg/m^3 of water, resulting in a water-to-cement ratio of 0.18, and included superplasticizer, Sika ViscoCrete PC HRF-2, and 2% steel fibres, as suggested by a previous study (Dupont & Vandewalle, 2005). The details of the mix design are presented in Table 1 and physical properties of rubber is provided in Table 2. Brass-coated steel fibres with 13 mm in length and 0.2 mm in diameter were used as shown in Fig. 1. The tensile strength was greater than 2,300 MPa and the corresponding elastic modulus of 200 GPa, as provided by the supplier.

3.2 Casting and Curing

The dry ingredients, including cement, silica sand, and silica fume, were thoroughly mixed in a pan mixer to ensure uniform distribution. Small amounts of pre-treated, surface-dried rubber were added at intervals to avoid clumping and ensure even distribution. Three-quarters of the required water was then added, and the ingredients were mixed for about 10 min or until the water was evenly distributed around the dry materials. At this stage, the mix was relatively dry with minimal clumping observed. The remaining quarter of the water was mixed with HRF-2 superplasticizer to allow for easy distribution. The water and superplasticizer solution were then added in intervals and mixed for a total of 15 min, transforming the dry and clumpy mix into a paste with a honey-like consistency. Finally, steel fibres were added at intervals and mixed for an additional 5 min to ensure even distribution. To minimize rubber floating and steel fibres sinking, low-intensity vibration was maintained during the pouring process.

After mixing all the ingredients, they were poured into moulds and allowed to cure at room temperature for 24 h. Once the initial curing process was finished, the samples were subjected to steam curing for 72 h at 70 °C. Afterwards, they were left in the steam room for an additional 24 h for gradual cooling.

3.3 Testing Apparatus

Density and compression tests were conducted on all cured cylindrical samples, which measured 100 (diameter)×200 (height) mm. The tests were performed in accordance with ASTM C138 (2017) and ASTM C39 (2020), respectively. A total of 12 samples were tested using an MCC8 compression testing station. Due to the high compressive strength of UHPC (136 MPa), the tops and bottoms of the cylinders were ground flat before undergoing compression testing. Conventional sulphur capping was not recommended (ASTM C39, 2020).

Flexural tests were conducted on 100×100×400 mm beams as per ASTM C1609 (2012), with a span length of 300 mm. The tests were conducted using an LDVT to measure the vertical mid-span deflection of the beams. The load was applied at a rate of 0.075 mm/min until mid-span deflection reached 0.33 mm and then
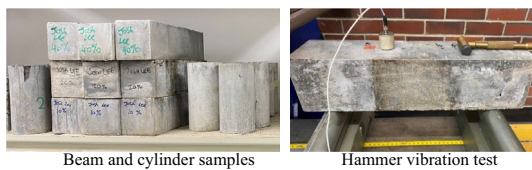
Pham *et al. Int J Concr Struct Mater*   (2024) 18:59

Page 7 of 15

Beam and cylinder samples   Hammer vibration test

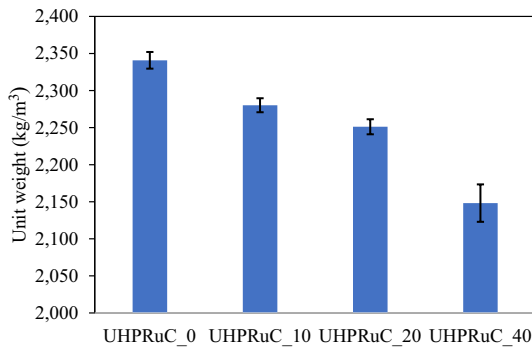**Fig. 3** Samples and vibration test setup

Fig. 4 Dry density of UHPRuC

increased to 0.2 mm/min until the specimen lost 50% of its strength.

The hammer vibration test was conducted on $100 \times 100 \times 400$ mm beams that were simply supported at a 300 mm span. The accelerometer is placed at the ¼ span of beams. An instrumented impulse hammer with a rubber head was used to induce vibrations of the beam, as shown in Fig. 3. The dominate vibration frequency component was identified using fast Fourier transformation and was decomposed from the overall vibration response using a band-pass filter. The filtered response was then used to determine the decaying rate by fitting the envelop line with negative decreasing exponential curve.

4 Experimental Results and Discussions
4.1 Dry Density
Fig. 4 shows the reductions in the dry density recorded according to ASTM C138 (2017). The control mix UHPRuC_0 had a density of 2341 kg/m³, and when the rubber content was increased to 10, 20, and 40% the density reduced to 2280 kg/m³, 2251 kg/m³ and 2148 kg/ m³, respectively. The dry density respectively reduced by 2.59%, 3.83%, and 8.23% regarding the reference UHPRuC_0. This is attributed to the replacement of silica sand with crumb rubber which had densities of 2343 kg/m³ and 1147 kg/m³, respectively. A non-linear decrease in the dry density may be caused by the uneven distribution of rubber aggregates and steel fibres. Despite

precautions during mixing and casting, buoyancy of rubber aggregates and sinking of steel fibres may lead to their uneven distribution within the sample.

Similarly, Elchalakani (2015) also found a decreasing dry density trend with increasing rubber content in the concrete mix increased, following a non-linear relationship. This trend may be attributed to the uneven distribution of rubber aggregates among the samples. The lack of uniform distribution of rubber aggregates and steel fibres, along with inconsistencies in determining the saturated surface dry conditions when using rubber aggregates, may have introduced errors during weighing. This could lead to excess water and reduced rubber content, ultimately impacting the density of concrete.

4.2 Failure Mode and Compressive Strength
ASTM C39 (2020) specifies six types of well-defined fracture patterns after compressive failure (see Fig. 5). UHPRuC_0 and UHPRuC_10 exhibited Type 3 fracture patterns with visible vertical cracking with no visible formed cones on both ends as shown in Fig. 6. UHPRuC_20 and R40UHPC showed a mix of Type 4 and 3 fracture patterns. UHPRuC_20 and UHPRuC_40 had visible columnar vertical cracks on both ends with no visible cones formed while also having detachable diagonal fractures on the samples. All the samples showed no visible Type 5 and Type 6 fracture patterns as they are the result of casting errors with an uneven top or bottom surface. In general, UHPRuC with a low rubber content failed with a columnar failure mode while those with higher rubber content ($\geq 20\%$) experienced a mixed failure mode associated with both vertical cracking and diagonal fracture.

Fig. 7 shows the results of the compression tests performed on UHPRuC with the rubber content ranging from 0 to 40%. It is noted that this study used the same mix design and reference samples of a previous study (Pham et al., 2021a). Therefore, the results of the compressive strength of these samples were also reported in the previous study while results on the flexural strengths and vibration characteristics, which were the primary objective of this work, have not been reported. The results show that the average compressive strength of UHPRuC_0 was 136.1 MPa, while UHPRuC_10, UHPRUC_20, and UHPRuC_40 had compressive strengths of 115.8 MPa, 103.8 MPa, and 67.7 MPa, respectively. This demonstrates a decrease in compressive strength with an increase in rubber content, UHPRuC exhibiting a 14.9% loss at 10% rubber content, a 23.7% loss at 20% rubber content, and a 50.2% loss at 40% rubber content. Despite of this reduction, UHPRuC_40 still displayed a high compressive strength of 68 MPa,
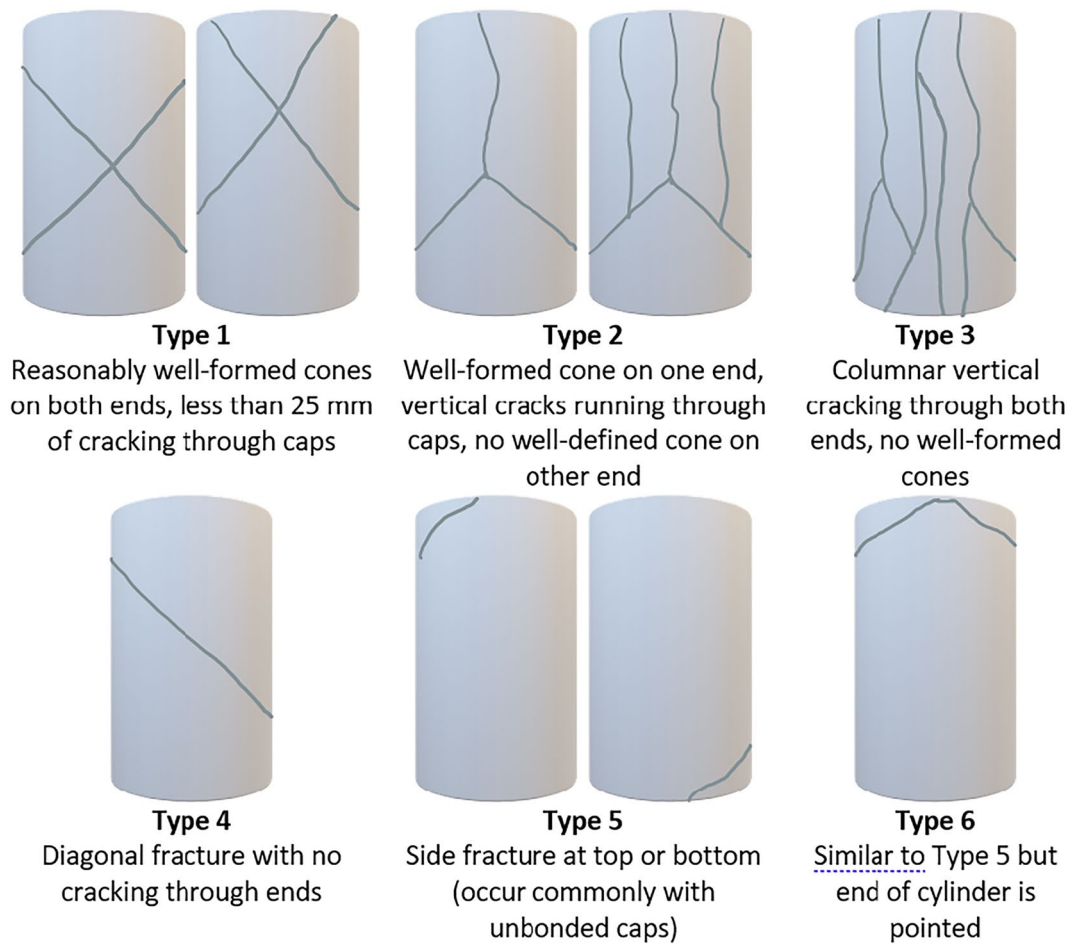
Pham *et al. Int J Concr Struct Mater*　　(2024) 18:59

Page 8 of 15

Fig. 5 Schematic of typical well-defined fracture patterns (ASTM C39 2020, 2019)

Type 1
Reasonably well-formed cones on both ends, less than 25 mm of cracking through caps

Type 2
Well-formed cone on one end, vertical cracks running through caps, no well-defined cone on other end

Type 3
Columnar vertical cracking through both ends, no well-formed cones

Type 4
Diagonal fracture with no cracking through ends

Type 5
Side fracture at top or bottom (occur commonly with unbonded caps)

Type 6
Similar to Type 5 but end of cylinder is pointed
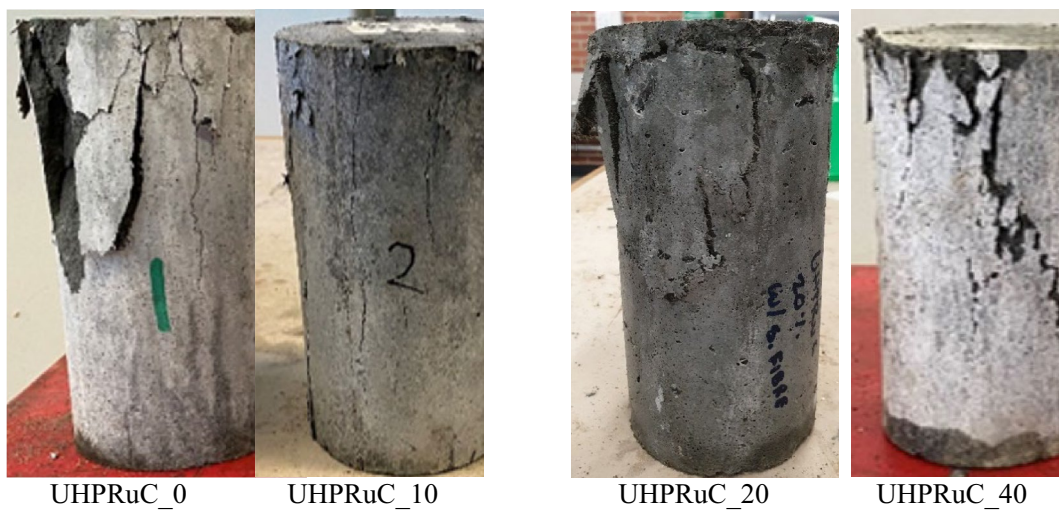

UHPRuC_0　　UHPRuC_10　　UHPRuC_20　　UHPRuC_40

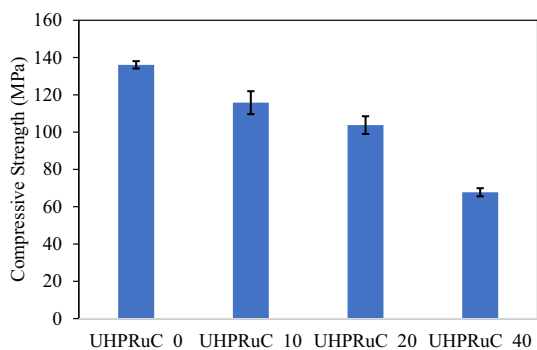**Fig. 6** Observed fracture patterns of UHPRuC

Fig. 7 Average compressive strength of UHPRuC

classifying it as high-strength concrete. As shown, the results almost follow a linear pattern, indicating that the compressive strength decreases linearly with the increase in rubber content. However, previous studies (Elchalakani, 2015; Eldin & Senouci, 1993) have suggested an exponential loss in compressive strength with an increase in rubber content, following Popovics's model of macro porosity. The loss in compressive strength is attributed to the low modulus of elasticity of rubber, which causes it to deform instead of bearing the load when subjected to external loads, effectively reducing the overall compressive strength.

This study found a lower strength loss compared to the previous studies (Elchalakani, 2015; Eldin & Senouci, 1992). These studies reported an average strength loss of 30% at 10% rubber content, 62% strength loss at 20%, and 84% strength loss at 40% (Audrius et al., 2012; Elchalakani, 2015). There are several possible explanations for the lower strength loss in this study. Firstly, the water soaking and washing pre-treatment process applied to the rubber aggregates may have reduced the strength loss compared to untreated rubber, as reported in the literature (Pham et al., 2019). Secondly, the reference mix used in this study had a compressive strength of 136 MPa, which is significantly higher than in previous studies and may have resulted in a stronger bond between rubber and matrix. Finally, this study used smaller rubber particles (0.6 mm) than previous studies, which has been shown to mitigate the strength loss as compared to those in Pham et al. (2021b).

Additionally, the strength loss in this study did not follow Popovics's model of macro porosity as observed in the previous studies (Elchalakani, 2015; Eldin & Senouci, 1993) because of the following two reasons. Firstly, this model was suggested for macro porosity of normal concrete which usually has a porosity of
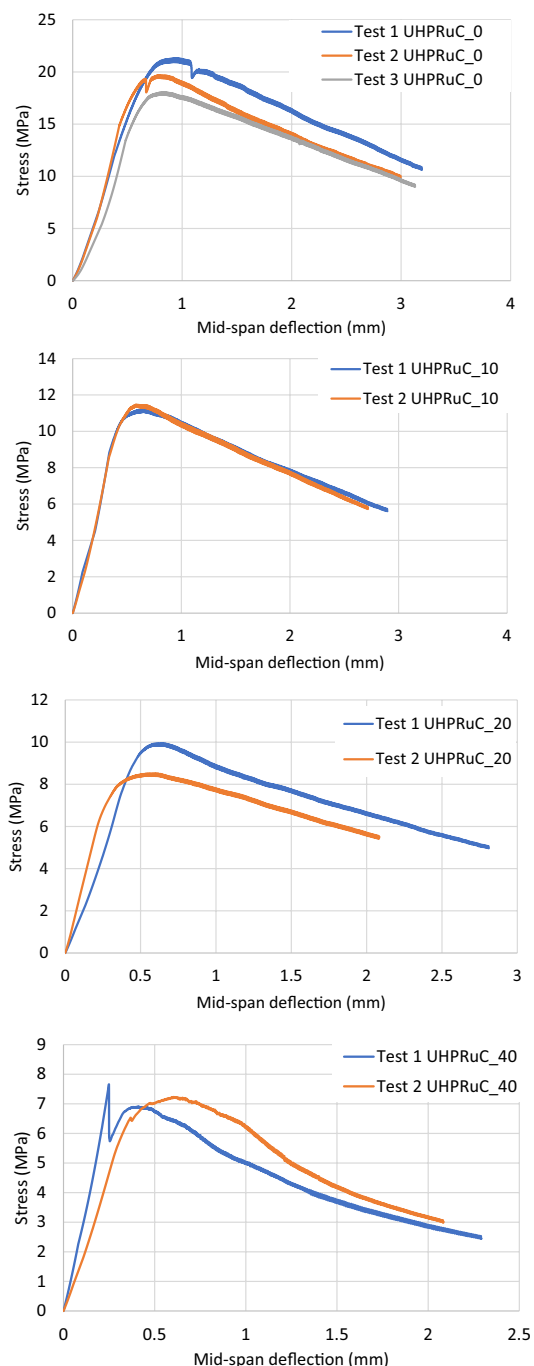

Fig. 8 Load–deflection curve of UHPRuC

up to 10–15% while the porosity of UHPC often falls in the range of 6% (Bahmani & Mostofinejad, 2022). Secondly, UHPC contains very small size void [e.g. < 0.01 mm (Frías and Cabrera 2000)] as compared to those of conventional concrete [e.g. 0.15–0.5 mm (Etxeberria et al., 2006)].

Table 3 Flexural strength of UHPRuC

Mix	Peak load (kN)		Flexural strength (MPa)		Disp. at peak stress (mm)	
	Mean	S. D	Mean	S. D	Mean	S. D
UHPRuC_0	43.46	2.73	19.56	1.23	0.83	0.06
UHPRuC_10	24.55	0.47	11.04	0.20	0.51	0.02
UHPRuC_20	20.50	1.58	9.23	0.71	0.62	0.04
UHPRuC_40	16.53	0.52	7.44	0.23	0.42	0.24

In general, the compressive strength of UHPRuC showed a smaller strength reduction as compared to conventional concrete with similar rubber content. This observation suggests that using reference concrete with a good bond strength of the matrix is an effective way to minimise the strength loss of rubberised concrete.

4.3 Flexural Properties

4.3.1 Flexural Strength

The experimental results of flexural tests are presented in Fig. 8 and Table 3. The flexural strength is calculated based on the peak applied force and Eq. 1. The control mix UHPRuC_0 had the flexural strength of 20 MPa which falls into the common range (15–35 MPa) but relatively a lower bound of similar strength UHPC (Huang et al., 2021). The relatively low flexural strength might be due to (1) the use of HRF-2 instead of HRF-1 superplasticizer, which is a newer generation of high range water reducer, (2) the use of pan mixer with low rotating speed as compared to other studies, and (3) lower temperature of the steam room at 70 degrees instead of 90 degrees as commonly adopted in the literature.

$$f_t = \frac{3FL}{2bh^2},\tag{1}$$

where f_t is the flexural strength, F is the maximum applied force in the three-point bending tests, L is the effective span, and b and h are the width and height of the beams, respectively.

UHPRuC_10, UHPRuC_20, and UHPRuC_40 had the flexural strength of 11.04 MPa, 9.23 MPa, and 7.44 MPa, respectively. The increase in rubber content had significantly reduced the flexural strength by 43.71%, 52.81%, and 61.96%, respectively. These strength losses are similar to the study by Ganjian et al. (2009) who reported a 50% loss in the flexural strength with 10% rubberised concrete. Meanwhile, Thomas and Gupta (2015) observed a lower loss in the flexural strength of 13% for 10% rubberised concrete and 17% for 20% rubberised concrete. The wide range in flexural strength

loss can be associated with different mix designs as these previous studies were associated with very different rubber sizes. Similar to the compressive strength, the loss in the flexural strength can be linked to the weak internal binding between the rubber aggregate and cement (Bušić et al., 2018).

Previous studies have observed different relationships between the flexural strength and rubber content. Benazzouk et al. (2007) observed an 18% maximum gain in the flexural strength with the optimum rubber content between 20 and 30%. When the rubber content exceeded 30%, a decrease in the flexural strength was observed. This decrease was attributed to the elastic behaviour of rubber under load, which caused the tensile strain energy to be redirected to the crumb rubber, reducing cracking and resulting in improved flexural strength (Benazzouk et al., 2007). For example, this current study found that UHPRuC_20 had a mid-span displacement of 0.62 mm at peak stress while the corresponding displacement of UHPRuC_10 was 0.51 mm. However, a significant reduction in the flexural strength of UHPRuC was observed in this study and this reduction rate was greater than that in the compressive strength.

The strength reduction rate of UHPRuC was different under compression and tension due to dissimilar influences of insufficient bonding of rubber particle under compression vs tension. Under compression, insufficiently bonded rubber particles cannot bear stress which is redistributed to surrounding particles. However, these weak points or discontinuities in a similar matrix have greater impact in tension, and thus, it could lower the flexural strength.

4.3.2 Residual Strength and Flexural Toughness

In UHPRuC, the matrix component primarily bears the load, while the role of the fibres is only activated when initial cracks occur in the concrete. After cracks initiate and develop in the matrix, and particularly post-peak load, the contribution of fibres become more prominent through the bridging effect. Accordingly, the residual strengths f_{600}^D, f_{300}^D, and f_{150}^D were adopted to examine the post-peak behaviour of UHPRuC. f_{600}^D, f_{300}^D, and f_{150}^D are the stress at deflection of $L/600$ (0.5 mm), $L/300$

Pham *et al. Int J Concr Struct Mater*   (2024) 18:59

Page 11 of 15

Table 4 Post-peak behaviour of UHPRuC

Mix	f_{300}^D(MPa)	f_{150}^D(MPa)	T_{300}^D(J)	T_{150}^D(J)
UHPRuC_0	19.09	14.56	28.34	65.88
UHPRuC_10	10.43	7.74	18.67	38.68
UHPRuC_20	8.32	6.12	15.61	31.56
UHPRuC_40	5.63	2.98	12.31	21.20

(1.0 mm), and L/150 (2.0 mm), respectively. In general, f_{600}^D is associated with the capacity of fibre reinforced concrete at the peak stage, f_{300}^D represents the early range of the post-peak region, and f_{150}^D is about the residual stress at the later stage deflection. These indices are recommended for four-point pending tests while this study conducted three-point bending tests due to availability of the equipment. Accordingly, f_{600}^D does not belong to the post-peak region so only f_{300}^D and f_{150}^D are discussed.

Table 4 summarises the corresponding results. As shown, increasing the rubber content in the UHPRuC led to a reduction in the post-peak strengths, e.g. f_{300}^D and f_{150}^D. Compared to UHPRuC_0, the residual strength f_{300}^D of UHPRuC_10, UHPRuC_20, and UHPRuC_40 reduced by 45%, 55%, and 70%, respectively. The reduction was at a relatively same rate as that of the peak flexural strength discussed above, for instance, the flexural strength of UHPRuC_10, UHPRuC_20, and UHPRuC_40, respectively, decreased by 44%, 53%, and 62% as compared to the reference mix. Thus, the addition of rubber aggregates to UHPC reduced the peak strength and residual strength at a relatively similar rate.

To evaluate the energy absorption capability of concrete, the flexural toughness is examined, and it is determined by the area under the load–deflection curve up to net deflection of L/300 (1.0 mm) and L/150 (2.0 mm) which is represented as T_{300}^D and T_{150}^D in Table 4. Similar to

the flexural strength, increasing the rubber content of UHPRuC decreased its flexural toughness. For example, the flexural toughness at L/150 (2.0 mm) of UHPRuC_0, UHPRuC_10, UHPRuC_20, and UHPRuC_40 reduced by 41%, 52%, and 68%, respectively, as compared to the reference mix. Overall, the addition of rubber aggregate in a UHPC reduced the peak flexural strength, residual strength, and flexural toughness at a relatively similar rate.

4.4 Free-Decay Vibration Responses

Typically, the energy of hammer impact load is dissipated by the structure system during the vibration and finally decay to zero. As shown in Fig. 9, the free-decay acceleration response of an underdamped vibration system is a cosine with time-decaying amplitude, and is expressed as

$$a(t) = A_0 \exp(-\lambda t)\cos(\omega_d t + \phi_0), \qquad (2)$$

where A_0 is the initial free-decay amplitude, which can be determined by the maximum vibration after the applied hammer load. ω_d and ϕ_0 denote the dominate vibration frequency and its corresponding initial phase angle, respectively. λ is the coefficient that is related to the decaying rate of vibration responses. In particular, a larger λ means that the vibration responses decay faster. Therefore, the decay rate λ can be employed to quantitively evaluate the energy dissipation capacity of concrete beams.

Hammer impact vibration tests were carried out on concrete beams where the accelerometer was attached at the ¼ span and an instrumented hammer with a rubber head was used to induce vibrations on the opposite ¼ span. All the beams were hit 4–5 times and the average dominate vibration frequency and decaying rate along with the corresponding standard deviation (SD) are reported in Fig. 10. The decaying rate λ defined in Eq. (1) is obtained by curve fitting the envelop line of vibration response.
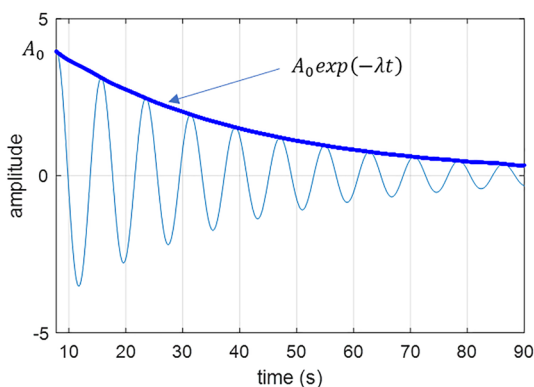

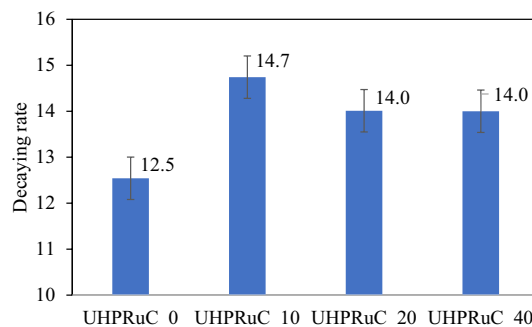**Fig. 9** Illustration of free-decay vibration responses

Fig. 10 Decaying rate of UHPRuC at ¼ span

Fig. 10 shows the experimental decaying rate results of all the tested samples. It is noted that the vibration decaying rate in this study has a similar physical meaning as the damping ratio reported in previous studies. UHPRuC_0 exhibited the lowest decaying rate at 12.5. It should be noted that the decaying rate can largely vary with the experimental setup and testing sample dimensions, and significant errors may exist in the identification process. Smaller samples with a more rigid and supportive test setup tended to have lower decaying rate for the same given mix with larger samples and less supportive setup (Wang et al., 2020). The test sample was a $400 \times 100 \times 100$ mm beam simply supported at 300 mm span which can be classified as a small sample with a moderate support system where relatively lower decaying rate can be expected.

The results of the decaying rate tests indicate that the implementation of rubber aggregates results in an increase in energy-dissipating capacity. This study showed that the highest average decaying rate increase was 17.6% for UHPRuC_10, followed by UHPRuC_20 and UHPRuC_40 with a 12% increase. The increase in rubber content, however, did not directly correspond to an increase in the energy-dissipating capacity. In fact, the highest energy-dissipating capacity was observed when the rubber content was 10%, followed by 40% and 20%. The increase of rubber content in concrete literally leads to improvement in the damping properties but a reduction in the mechanical properties. The final vibration characteristic of rubberised concrete depends on these inter-related factors and the results from this study demonstrated that UHPRuC_10 possessed the highest vibration decaying rate.

This trend was similar to the findings by Zheng et al. (2008), who found that the increase in damping ratio was highest for rubber content ranging from 0 to 30%, but decreased from 30 to 45%. The decrease in damping ratios or energy-dissipating capacity with higher rubber content was likely due to the ineffective interaction between cement and the increased rubber content in the mix design. Similarly, other studies (Habib et al., 2020; Xue & Shinozuka, 2013), conducted on similar-size rubber content, also observed a direct increase in the damping ratio with an increase of rubber content up to 20% replacement.

The current literature on the relationship between rubber aggregates and damping ratio in rubberized concrete is somewhat inconsistent, with some studies finding that larger rubber aggregates lead to a direct increase in damping ratio with an increase in rubber content, while smaller crumb rubber aggregates show an increase in damping ratio until a certain threshold in rubber content, after which a downward trend is observed. The present study observed a similar trend, the energy-dissipating capacity increased with rubber content up to 10%, and a higher rubber content did not show an improvement in the energy-dissipating capacity. The non-uniform distribution of steel fibres and air voids may have contributed to inconsistencies in the results. Further research is needed to fully understand the interaction between rubber content in UHPC and the resulting damping ratios.

5 Embodied Carbon Dioxide Emissions

The primary objective of this study is two folds, e.g. incorporating small rubber particles as aggregates of UHPC to resolve the negative environmental impact of rubber waste while minimising its negative impact on the compressive strength and improving the damping effect. To examine the environmental impact of this UHPRuC, the total embodied carbon dioxide emissions ($e\mathrm{CO}_2$) of raw materials and production is estimated. Table 5 provides an overview of the $e\mathrm{CO}_2$ coefficients for the initial components, as adopted from previous studies (Mohana & Bharathi, 2023; Park et al., 2021; Shi et al., 2019; Wiedmann et al., 2019). The use of rubber particles in concrete saves them from being burning as waste processing. Accordingly, the $e\mathrm{CO}_2$ can be offset from burning tyres. The embodied CO_2 emission of burning rubber tyres is the amount of carbon dioxide that is released into the atmosphere when tyres are incinerated for energy or disposal. According to United States Environmental Protection Agency (2006), the energy content per passenger tyre is about 0.25 MMBtu, and the carbon coefficient is 0.08 MTCO$_2$/MMBtu. This means that burning one passenger tyre would emit about 0.02 MTCO$_2$, or 20 kg of CO_2. The weight of a typical tyre can range between 6.8 and 11.3 kg. The range of $e\mathrm{CO}_2$ emission per kilogramme of rubber tyre being burnt is between 1.77 and 2.94 kg CO_2/kg. However, this does not account for the emissions from transporting,

Table 5 Embodied carbon dioxide emissions of materials

Raw material	Silica Sand	30-mesh rubber	Cement	Superplasticizer	Silica Fume	Steel Fibre	Water	Burning rubber tyre	Heat curing (kgCO$_2$/m^3)
$(e\mathrm{CO}_2)_i$ (kgCO$_2$/kg)	0.0100	0.0040	0.8300	0.7200	0.0140	1.4965	0.0003	-2.3550	189.2400

processing, and handling the tyres before and after combustion. There was no segregation issue during the mixing process. The heat curing of UHPC for 3 days was expected to emit $189.24 \frac{kgCO_2}{m^3}$ (Tran et al., 2023).

In this research, the overall (eCO_2) for a UHPC blend was calculated as the total of carbon dioxide emissions originating from its constituent materials. This calculation was achieved by multiplying the eCO_2 coefficients $(eCO_2)_i$ associated with each component by their respective quantities (m_i) within one cubic metre of the UHPC, as depicted in Eq. (3).

$$eCO_2 = \sum (eCO_2)_i m_i - 2.355\,m_{rubber}. \tag{3}$$

The eCO_2 of UHPRuC_40 showed a significant reduction up to 37% while the UHPRuC still exhibited good mechanical properties and even better damping behaviour as compared to the reference mix.

6 Conclusions

This study investigated the material properties of ultra-high-performance rubberised concrete (UHPRuC) and found the following key results:

1. The dry density of UHPRuC decreased non-linearly with an increase in the rubber content.
2. UHPRuC with a low rubber content failed with a columnar failure mode, while those with higher rubber content ($\geq 20\%$) experienced a mixed failure mode with both vertical cracking and diagonal fracture.
3. The compressive strength of UHPRuC up to 40% replacement showed a smaller strength reduction compared to conventional concrete with similar rubber content, mitigating the strength reduction approximately 50% as compared to previous studies. Using reference concrete with good bond strength is effective in minimising the strength loss of rubberised concrete.
4. Even though effective in mitigating compressive strength reduction, the use of UHPC could not minimise loss in flexural strength, 1.5–3 times of loss in compressive strength.
5. The addition of rubber aggregate in UHPC reduced the peak flexural strength, residual strength, and flexural toughness with a relatively similar rate.
6. The incorporation of rubber aggregates resulted in an increase in vibration decaying rate, with the highest average increase being 17.5% for UHPRuC_10, followed by UHPRuC_40 and UHPRuC_20 with a 12% increase.
7. Incorporating 40% rubber in UHPRuC reduced the eCO_2 up to 37% as compared to the reference UHPC.

Overall, this study found that while the addition of rubber aggregate in UHPC leads to reductions in strength, it also increases vibration decaying rate (up to a threshold), and using reference concrete with good bond strength can help minimize the strength loss.

Author contributions
Thong M. Pham contributed to writing—review and editing, supervision, resources, methodology, funding acquisition, and conceptualisation. Josh Lee was involved in methodology, investigation, formal analysis, and data curation. Emad Pournasiri, Jun Li, and Zhen Peng performed investigation, formal analysis, and data curation. Kaiming Bi and Tung M. Tran were involved in writing—review and editing.

Availability of data and materials
All data are presented in this manuscript.

Declarations

Ethics approval and consent to participate
Not applicable.

Consent for publication
The authors give consent to the publisher for publication.

Competing interests
The authors declare no competing interests.

References
Abdelmonem, A., El-Feky, M. S., Nasr, E. S. A. R., & Kohail, M. (2019). Performance of high strength concrete containing recycled rubber. *Construction and Building Materials, 227*, 116660.
ASTM C1609. (2012). *Flexural performance of fiber-reinforced concrete (using beam with third-point loading). ASTM C1609/C1609M-12*. ASTM International.
ASTM C138. (2017). *C138/C138M-17a standard test method for density (unit weight), yield, and air content (gravimetric) of concrete*. ASTM International.
ASTM C39. (2020). *C39/C39M-20 standard test method for compressive strength of cylindrical concrete specimens*. ASTM International.
Audrius, G., Henrikas, S., & Mindaugas, D. (2012). Tyre rubber additive effect on concrete mixture strength. *Journal of Civil Engineering and Management, 18*(3), 393–401.
Bahmani, H., & Mostofinejad, D. (2022). Microstructure of ultra-high-performance concrete (UHPC)—a review study. *Journal of Building Engineering, 50*, 104118.
Bakhoum, E. S., & Mater, Y. M. (2022). Decision analysis for the influence of incorporating waste materials on green concrete properties. *International Journal of Concrete Structures and Materials, 16*(1), 63.
Benazzouk, A., Douzane, O., Langlet, T., Mezreb, K., Roucoult, J. M., & Quéneudec, M. (2007). Physico-mechanical properties and water absorption of cement composite containing shredded rubber wastes. *Cement and Concrete Composites, 29*(10), 732–740.
Bušić, R., Miličević, I., Šipoš, T. K., & Strukar, K. (2018). Recycled rubber as an aggregate replacement in self-compacting concrete-literature overview. *Materials (basel), 11*(9), 1729.

Pham *et al. Int J Concr Struct Mater*   (2024) 18:59

Page 14 of 15

Cement Concrete and Aggregates Australia. (2022). Concrete overview. https://www.ccaa.com.au/CCAA/CCAA/Public_Content/INDUSTRY/Concrete/Concrete_Overview.aspx?hkey=44d42eeb-2621-4e4b-abbb-932e5946e2cd. Accessed 21 Nov 2022.

Chan, Y.-W., & Chu, S.-H. (2004). Effect of silica fume on steel fiber bond characteristics in reactive powder concrete. *Cement and Concrete Research, 34*(7), 1167–1172.

Chou, L. H., Lu, C.-K., Chang, J.-R., & Lee, M. T. (2007). Use of waste rubber as concrete additive. *Waste Management & Research, 25*(1), 68–76.

Dupont, D., & Vandewalle, L. (2005). Distribution of steel fibres in rectangular sections. *Cement and Concrete Composites, 27*(3), 391–398.

Elchalakani, M. (2015). High strength rubberized concrete containing silica fume for the construction of sustainable road side barriers. *Structures, 1*, 20–38.

Eldin, N. N., & Senouci, A. B. (1992). Engineering properties of rubberized concrete. *Canadian Journal of Civil Engineering, 19*(5), 912–923.

Eldin, N. N., & Senouci, A. B. (1993). Observations on rubberized concrete behavior. *Cement, Concrete and Aggregates, 15*(1), 74–84.

El-Helou, R. G., Haber, Z. B., & Graybeal, B. A. (2022). Mechanical behavior and design properties of ultra-high-performance concrete. *ACI Materials Journal, 119*(1), 181–194.

Elsayed, M., Tayeh, B. A., Taha, Y., & El-Azim, A. A. (2022). Experimental investigation on the behaviour of crumb rubber concrete columns exposed to chloride–sulphate attack. *Structures, 46*, 246–264.

Etxeberria, M., Vázquez, E., & Mari, A. (2006). Microstructure analysis of hardened recycled aggregate concrete. *Magazine of Concrete Research, 58*, 683–690.

Feng, L.-Y., Chen, A.-J., & Liu, H.-D. (2021). Effect of waste tire rubber particles on concrete abrasion resistance under high-speed water flow. *International Journal of Concrete Structures and Materials, 15*(1), 37.

Feng, L.-Y., Chen, A.-J., & Liu, H.-D. (2022). Experimental study on the property and mechanism of the bonding between rubberized concrete and normal concrete. *International Journal of Concrete Structures and Materials, 16*(1), 25.

Frías, M., & Cabrera, J. (2000). Pore size distribution and degree of hydration of metakaolin–cement pastes. *Cement and Concrete Research, 30*(4), 561–569.

Ganjian, E., Khorami, M., & Maghsoudi, A. A. (2009). Scrap-tyre-rubber replacement for aggregate and filler in concrete. *Construction and Building Materials, 23*(5), 1828–1836.

Gesoglu, M., & Guneyisi, E. (2007). Strength development and chloride penetration in rubberized concretes with and without silica fume. *Materials and Structure, 40*, 953–964.

Gravina, R. J., Xie, T., Roychand, R., Zhuge, Y., Ma, X., Mills, J. E., & Youssf, O. (2021). Bond behaviour between crumb rubberized concrete and deformed steel bars. *Structures, 34*, 2115–2133.

Habib, A., Yildirim, U., & Eren, O. (2020). Mechanical and dynamic properties of high strength concrete with well graded coarse and fine tire rubber. *Construction and Building Materials, 246*, 118502.

Holmes, N., Dunne, K., & O'Donnell, J. (2014). Longitudinal shear resistance of composite slabs containing crumb rubber in concrete toppings. *Construction and Building Materials, 55*, 365–378.

Huang, H., Gao, X., & Khayat, K. H. (2021). Contribution of fiber alignment on flexural properties of UHPC and prediction using the Composite Theory. *Cement and Concrete Composites, 118*, 103971.

Jafarifar, N., Bagheri Sabbagh, A., & Uchehara, I. (2023). Rubberised concrete confined with thin-walled steel profiles; a ductile composite for building structures. *Structures, 49*, 983–994.

Li, H., Tu, H., & Weng, Y. (2022). Investigation on the quasi-static mechanical properties and dynamic compressive behaviors of ultra-high performance concrete with crumbed rubber powders. *Materials and Structures, 55*(3), 1–16.

Li, W., Huang, Z., Wang, X., and Wang, J. (2014). Review of crumb rubber concrete. Applied Mechanics and Materials, 672–674(Renewable Energy and Power Technology II), 1833–1837.

Marinković, S., Radonjanin, V., Malešev, M., & Ignjatović, I. (2010). Comparative environmental assessment of natural and recycled aggregate concrete. *Waste Management (oxford), 30*(11), 2255–2264.

Mohana, R., & Bharathi, S. M. L. (2023). Sustainable approach of promoting impact resistant rubberized geopolymer by reducing the embodied emission rate of climate changing substances. *Structures, 57*, 105241.

Mountjoy, E., & Mountjoy, G. (2012). *Study into domestic and international fate of end-of-life tyres-final report*. Hyder Consulting Pty Ltd.

Najim, K. B., & Hall, M. R. (2010). A review of the fresh/hardened properties and applications for plain- (PRC) and self-compacting rubberised concrete (SCRC). *Construction and Building Materials, 24*(11), 2043–2051.

Najim, K., & Hall, M. (2013). Crumb rubber aggregate coatings/pre-treatments and their effects on interfacial bonding, air entrapment and fracture toughness in self-compacting rubberised concrete (SCRC). *Materials and Structures, 46*(12), 2029–2043.

Onuaguluchi, O., & Banthia, N. (2017). Durability performance of polymeric scrap tire fibers and its reinforced cement mortar. *Materials and Structures, 50*(2), 158.

Park, S., Wu, S., Liu, Z., & Pyo, S. (2021). The role of supplementary cementitious materials (SCMs) in ultra high performance concrete (UHPC): A review. *Materials, 14*(6), 1472.

Pham, T. M., Chen, W., Khan, A. M., Hao, H., Elchalakani, M., & Tran, T. M. (2020). Dynamic compressive properties of lightweight rubberized concrete. *Construction and Building Materials, 238*, 117705.

Pham, T. M., Davis, J., Ha, N. S., Pournasiri, E., Shi, F., & Hao, H. (2021a). Experimental investigation on dynamic properties of ultra-high-performance rubberized concrete (UHPRuC). *Construction and Building Materials, 307*, 125104.

Pham, T. M., Elchalakani, M., Hao, H., Lai, J., Ameduri, S., & Tran, T. M. (2019). Durability characteristics of lightweight rubberized concrete. *Construction and Building Materials, 224*, 584–599.

Pham, T. M., Renaud, N., Pang, V. L., Shi, F., Hao, H., & Chen, W. (2021b). Effect of rubber aggregate size on static and dynamic compressive properties of rubberized concrete. *Structural Concrete, 23*(4), 2510–2522.

Portland Cement Association. (2023). Ultra-High Performance Concrete. https://www.cement.org/learn/concrete-technology/concrete-design-production/ultra-high-performance-concrete.

Pournasiri, E., Pham, T. M., & Hao, H. (2022a). Behaviour of ultra-high performance concrete (UHPC) bridge decks with new Y-shape FRP stay-in-place formworks. *Journal of Composites for Construction, 26*(3), 04022023.

Pournasiri, E., Pham, T. M., & Hao, H. (2022b). Structural performance evaluation of UHPC/conventional concrete cast on novel FRP stay-in-place formwork for concrete bridge decks. *Structures, 41*, 1077–1091.

Raffoul, S., Garcia, R., Pilakoutas, K., Guadagnini, M., & Medina, N. F. (2016). Optimisation of rubberised concrete with high rubber content: An experimental investigation. *Construction and Building Materials, 124*, 391–404.

Shi, Y., Long, G., Ma, C., Xie, Y., & He, J. (2019). Design and preparation of ultra-high performance concrete with low environmental impact. *Journal of Cleaner Production, 214*, 633–643.

StandardsAustralia. (2018). *AS 3600:2018 concrete structures*. SAI Global.

Su, H., Yang, J., Ling, T.-C., Ghataora, G. S., & Dirar, S. (2015). Properties of concrete prepared with waste tyre rubber particles of uniform and varying sizes. *Journal of Cleaner Production, 91*, 288–296.

Sun, S., Han, X., Chen, A., Zhang, Q., Wang, Z., & Li, K. (2023). Experimental analysis and evaluation of the compressive strength of rubberized concrete during freeze-thaw cycles. *International Journal of Concrete Structures and Materials, 17*(1), 28.

Thomas, B. S., & Gupta, R. C. (2015). Long term behaviour of cement concrete containing discarded tire rubber. *Journal of Cleaner Production, 102*, 78–87.

Tran, T. M., Trinh, H. T., Nguyen, D., Tao, Q., Mali, S., & Pham, T. M. (2023). Development of sustainable ultra-high-performance concrete containing ground granulated blast furnace slag and glass powder: Mix design investigation. *Construction and Building Materials, 397*, 132358.

Tyre recycle. (2018). www.tyrecycle.com.au/. Accessed 27 June 2018.

United States Environmental Protection Agency (2006). Life-cycle greenhouse gas emission factors for scrap tires. https://19january2017snapshot.epa.gov/www3/epawaste/conserve/tools/warm/pdfs/ScrapTires5-9-06.pdf. Accessed 11 Oct 2023.

Wang, Z., Wang, J., Zhu, J., Zhao, G., & Zhang, J. (2020). Energy dissipation and self-centering capacities of posttensioning precast segmental ultra-high performance concrete bridge columns. *Structural Concrete: Journal of the FIB, 21*(2), 517–532.

WBCSD. (2010). *End-of-Life Tires: A framework for effective management systems*. Wold Bussiness Council for Sustainable Development.

Wiedmann, T., Teh, S., & Yu, M. (2019). *ICM database-integrated carbon metrics embodied carbon life cycle inventory database*. University of New South Wales.

Xue, J., & Shinozuka, M. (2013). Rubberized concrete: A green structural material with enhanced energy-dissipation capability. *Construction and Building Materials, 42*, 196–204.

Zheng, L., Sharon Huo, X., & Yuan, Y. (2008). Experimental investigation on dynamic properties of rubberized concrete. *Construction and Building Materials, 22*(5), 939–947.

Publisher's Note

Thong M. Pham   Associate Professor at the University of South Australia, Australia.

Josh Lee   Graduate Engineer at the GHD Pty Ltd, Australia.

Emad Pournasiri   PhD candidate and structural engineer at the Curtin University and Parma Composites, Australia.

Jun Li   Professor at the Curtin University, Australia.

Zhen Peng   Research Fellow at the Curtin University, Australia.

Kaiming Bi   Associate Professor at the The Hong Kong Polytechnic University, China.

Tung M. Tran   Lecturer at the Ton Duc Thang University, Vietnam.